Identification of Potential Peptide Inhibitors of ACE-2 Target of SARS-CoV-2 from Buckwheat & Quinoa

Ashok Nanjaiah Rangaswamy[1] · Arpitha Ashok[1] · Pradeep Hanumanthappa[1] ·
Aparanji Sinduvalli Chandrashekaramurthy[1] · Monika Kumbaiah[1] · Pratibha Hiregouda[1] · Vaishali Sharma[1] ·
Aparna Huligerepura Sosalegowda[1]

Abstract
It is well established fact that peptides from various foods offer human health benefits displaying diverse functionalities. Millets considered as super foods is a major alternative in recent days for traditional diet being rich in proteins and fibre along with trace minerals and vitamins. In this connection, proteins from Buckwheat and Quinoa were digested by in vitro simulation digestion for the generation of peptides, analyzed by nLC-MS/MS and the functional annotations of the identified proteins/peptides were carried out. The study led to the identification of 34 small peptides and their parent proteins clustered into 4 gene functional groups and their localization prediction indicated their involvement in energy metabolism, transport and storage. Interestingly, the identified peptides maximally displayed DPP-IV and ACE inhibitions. The present study was extended to unravel ACE-2 inhibition targeting COVID-19 by selecting ACE-2-Spike binding domain for molecular docking studies. The NWRTVKYG interacted with the ACE-2-Spike interface displaying the feasible binding energy (− 213.63) and docking score (− 12.43) and the MD simulation revealed the ability of the peptide in stabilizing the protein-peptide composite. The present investigation thus establishes newer vista for food derived peptides having ACE-2 inhibitory potential as tentative strategy for SARS-CoV-2 therapeutics.

Keywords Peptides · nLC-MS/MS · Functional annotation · ACE-2 · Molecular dynamics

Introduction

The proficiency of diet-derived bioactive peptides in maintaining health is a well-researched niche in contemporary food science (Li-Chan 2015; Lafarga and Hayes 2017; Chakrabarti et al. 2018; Li et al. 2018a). The encrypted peptide sequences reveal their physiological function/bioactivity beyond conventional nutrition once they are released from their native proteins through enzymatic hydrolysis, digestion, fermentation or other food-processing techniques (Nongonierma and FitzGerald 2018). Hence, considerable research has been done to identify and establish the structure-function relationship of peptides with different bioactivities and even the possibility of multi-functional peptides, although, there are still considerable gaps yet to be validated.

Food protein-derived bioactive peptides have been reported to possess antioxidant (Hou et al. 2019), immunomodulatory (Chalamaiah et al. 2018), antihypertensive (Bhat et al. 2017), anti-inflammatory (Meram and Wu 2017), anti-microbial (Mohanty et al. 2016), hypocholesterolaemic (Nagaoka 2019), anti-diabetic (Admassu et al. 2018), anti-cancer properties (Díaz-Gómez et al. 2017), among various others. Hence, there is considerable interest in development of peptides for commercial use as additives or functional food products/nutraceuticals, which can improve human health for specific or generic use (Chalamaiah et al. 2019).

Until recently, the most-exploited sources for bioactive peptides include milk, milk products and other animal-based sources of protein. Currently, researchers focus on exploring novel and under-utilised sources of plant origin. Pseudo-cereals comprise of one such group that has gained attention since FAO's predicament as one of the key resources for food security (FAOSTAT 2018; Morales et al. 2020).

✉ Aparna Huligerepura Sosalegowda
hsa.uom@gmail.com

1   Department of Studies in Biotechnology, University
     of Mysore, Manasagangothri, Mysore, Karnataka 570 006,
     India

"Pseudocereals" refer to the under-utilized foods that differ from " true" cereals in bearing dicotyledonous seeds as compared to the monocotyledonous cereals, but these resemble cereals with features like starch content, texture, palatability and cooking methods (Schoenlechner et al. 2008; Ciudad-Mulero et al. 2019). Some of the popular and most reviewed pseudocereals are Quinoa (*Chenopodium quinoa*), amaranth (*Amaranthus* spp.), chia (*Salvia hispanica*) and Buckwheat (*Fagopyrum* spp.). Pseudocereals are known for their high nutritional value naturally supplemented with high quality proteins complete with essential amino acids like lysine.

Buckwheat is a common term referring to the genus *Fagopyrum* of family *Polygonaceae. Fagopyrum esculentum* Moench., (Common or Japanese Buckwheat) and *Fagopyrum tataricum* Gaertin., (Tatary Buckwheat) are the most widely cultivated species under the genus. The protein content of Tartary Buckwheat ranges between 8 and 19% comprising of albumin (51.52%), globulin (13.69%) and gliadin (8.83%) (Zhu 2016). In Asia, Buckwheat is also traditionally cultivated for its medicinal properties having beneficial bioactive compounds like proteins, flavonoids, polysaccharides, saponins, polyphenols and fatty acids that are known to decrease the risk factors associated with cancer, cardiovascular diseases or hepatic problems (Ji et al. 2019). Tartary Buckwheat is also known to reduce the incidence of hyperglycemia, hypertension and hyperlipidemia; efficiently avert and treat diabetes (Ruan et al. 2020). It is also considered as an ideal health food for adults and the elderly.

Quinoa (*Chenopodium quinoa*, Willd) is a pseudocereal native to the Andean regions of South America, currently cultivated mostly in Asia and Europe (FAOSTAT 2018). It belongs to Amaranthaceae family, Subfamily Chenopodioideae and the genus *Chenopodium*. Like Buckwheat, Quinoa too is renowned for its superior protein content being among the few crops with all the essential amino acids (Nascimento et al. 2014). Quinoa is nutritionally rich compared to grains in terms of protein, lipids and ash content (Hernández-Ledesma 2019). The protein content in Quinoa seeds ranges from 13.8 to 16.5% (Navruz-Varli and Sanlier 2016), majorly comprising of globulins (37%), albumins (35%), and prolamins in low concentrations (Abugoch James 2009). Quinoa is an excellent protein source capable of providing up to 180% of required protein for adults (Comai et al. 2007). In addition, it is also characterized by protein content that has high-bioavailability, and high digestability (Ruales et al. 2002; Vega-Gálvez et al. 2010) attribute Quinoa with potential for use as functional foods and nutraceuticals (Hernández-Ledesma 2019).

The research on Quinoa as a source for bioactive peptides is still in its infancy, although few studies have already explored the anti-oxidant (Aluko and Monu 2003; Nongonierma et al. 2015; Rizzello et al. 2017), anti-hypertensive (Aluko and Monu 2003), hypocholesterolaemic (Takao et al. 2005), anti-diabetic (Vilcacundo et al. 2017), chemopreventive (Vilcacundo et al. 2018) properties of Quinoa protein hydrolysates; however, only few studies identified the peptides responsible for the proposed bioactivities (Rizzello et al. 2016; Vilcacundo et al. 2017, 2018; Li et al. 2018a, b).

Hence, owing to the rich and high-quality protein content, along with already reported health benefits, both Buckwheat and Quinoa have excellent potential to be investigated for novel bioactivities. Although food proteins have been extensively profiled for ACE-inhibition and anti-oxidant efficacy, few/no reports have evaluated food-derived bioactive peptide inhibitors for ACE-2, a key enzyme in RAS as well as the current tentative strategy for SARS-CoV-2 therapeutics.

Angiotensin Converting enzyme-2 (ACE-2) is an important factor in the renin-angiotensin system (RAS) which catalyzes the cleavage of leucine from the C-terminus of Ang I to form the biologically active peptide Ang (1–9) (Santos et al. 2013). However, of late, ACE-2 has gained significant attention for it being a functional receptor for the SARS coronavirus, and in particular, the SARS-CoV-2; and it has been hypothesized that inhibition of the interaction of spike protein of SARS-CoV-2 ACE-2 can be an effective strategy to treat patients with COVID-19 (Chen et al. 2020; Monteil et al. 2020). Furthermore, ACE-2 receptor is known to be highly expressed on the mucosa of oral cavity, especially enriched in the epithelial cells of the tongue (Xu et al. 2020a). These recent findings suggest the ACE-2 to be a viable therapeutic target for exploring diet-based peptide inhibitors. Hence in the present investigation, through gastrointestinal simulation digestion both Buckwheat and Quinoa proteins were proteolytically digested, analysed and the peptides were exploited to unravel their efficacy for ACE-2 inhibition.

Materials and Methods

Materials

Buckwheat seeds, Quinoa seeds were purchased from the retail store, Mysore. Tris-HCl, Bovine Serum Albumin (BSA), Pepsin, Pancreatin, Tryptone, 2, 2′-azino-bis(3-ethylbenzothiazoline-6-sulphonic acid, ABTS), Potassium persulphate were purchased from Sigma Aldrich. All other reagents were either HPLC or analytical grade.

Methods

Total Protein Extraction from Buckwheat & Quinoa Flour

The seeds were washed thrice and rinsed with distilled water, kept for air drying over night followed by drying at 50 °C for 2 h. Both the seeds were then ground to flour

and dehusked. The flours were dispersed in Chloroform and Methanol mixture (1:2) and kept on magnetic stirrer for 2 h for defatting. Defatted flours were air dried overnight. Flour was dispersed in 50mM buffer (Tris-HCl, pH8) in the ratio 1:3 and slurry was subjected to sonication for 30 min and kept on magnetic stirrer at 4 °C for 4–5 h and centrifuged (10,000 rpm, 30 min, 4 °C) and the supernatant was vacuum concentrated and stored at 4 °C (Yang et al. 2014). Protein concentration was measured by Lowry's method using BSA as standard. SDS-PAGE analysis (12%) was performed as described by Nielsen and Reynolds 1978.

In Vitro Gastrointestinal Digestion and Ultrafiltration

The total protein of both Buckwheat and Quinoa suspended (3.5%, w/v) in KCl–HCl buffer (0.1 M, pH2) with pepsin (4%, w/w) were incubated for 4 h at 37 °C. Reaction was terminated by heating for 10 min followed by neutralization to pH 7 (2 N NaOH). The suspension was further digested by pancreatin (4%, w/w) for 4 h at 37 °C (Tsai et al. 2008). The enzyme was heat inactivated; centrifuged (10,000× g, 30 min) and the supernatants collected were filtered using MWCO membrane (3 kDa). The permeate collected were desalted using C-18 solid phase extraction disks (Ashok and Aparna 2017) and the peptides were quantified (Church et al. 1983).

Evaluation of Free Radical Scavenging Activity

ABTS radicals (ABTS*) were generated by reacting ABTS (7mM) with 2.45mM potassium persulphate. The mixture was kept in dark for 16 h at RT and the resultant mixture was diluted with PBS (150mM, pH 7.5) to give an absorbance of 0.7 at 734nm. The reaction was initiated by adding test samples (50 µl) to ABTS (950 µl). The mixture was incubated for 5 min at RT and the absorbance was measured at 734nm (Re et al. 1999). The percent inhibition was calculated using the following equation.

$$\text{Inhibition}(\%) = \frac{\text{A Control} - \text{A Test}}{\text{A Control} \times 100}$$

IC_{50} value of sample required to scavenge 50% of free radical was calculated.

Mass Spectrometry Deployed Peptide Characterization & Protein Identification

High Resolution Nano LC-MS/MS Analysis The samples were resolved on Agilent 6550 iFunnel QTOF mass spectrometer (Agilent Technologies) coupled to an Agilent 1260 Infinity Capillary Pump and 1260 Infinity Nanoflow Pump LC system. The samples (10 µl) were loaded on to a ProteinID-Chip (PepMap RSLC C18 2 µm, 100 A × 50 cm) via an Infinity Auto sampler (Low FlowHip Sampler, Agilent Technologies) using buffer A (0.1% formic acid in spectroscopic grade water) at a flow rate of 4 µl/min of Capillary Pump and 0.3 µl/min of nano Pump. Peptides were resolved using a linear gradient with initial conditions of 3% buffer B (90% acetonitrile containing 0.1% formic acid) increasing up to 98% buffer B in 20 min. Samples were introduced to the mass spectrometer through Agilent 1260 Chip-cube operating in ESI-positive and the precursor ions (350–3200 m/z) were selected for MS/MS with a threshold absorbance count of above 2000.

MS/MS Data Analysis The acquired data exported as .mgf files was processed in Agilent Mass Hunter Spectrum Mill MS Proteomics Workbench software (Version B.04.00.127). The sequences and their proteins were identified using MS/MS search option with enzyme specificity as Pepsin and Pancreatin against NCBInr protein database of *Zea mays*.

Gene Ontology Annotation, STRING 10 and Psort Analysis Gene ontology annotation was carried out using the Database for Annotation, Visualization and Integrated Discovery (DAVID) v6.7 (Benjamini and Hochberg 1995). All the identified proteins GI numbers were listed and converted into gene ID's using DAVID v6.7 and analyzed using Functional Annotation tool. Each gene cluster was viewed on a 2-D heatmap with green area representing highly common annotations and blackgreen area indicating differences in annotations. Sequences of all the proteins from Buckwheat and Quinoa were uploaded into Psort software (Nakai and Horton 1999) and the prediction of their Localization was done under default model in plant version. Protein-Protein interaction was decoded from STRINGv10 (Search Tool for the Retrieval of Interacting Genes/Proteins) database (http://string-db.org/) and the predicted association evidences of interacting proteins were sorted by combined confidence score of 0.99.

Investigation of Bioactivity Profiles of Generated Peptides using BIOPEP Database In order to assess the bioactive profile of peptides derived from Buckwheat and Quinoa, BIOPEP tool was employed through the "profiles of bioactivity" option (http://www.uwm.edu.pl/biochemia/index.php/en/biopep).

Protein Preparation and Binding Site Prediction

X-ray crystal structure of the ACE-2 in complex with co-crystallized protein: spike, PDB ID:6MOJ was fetched from RCSB database (https://www.rcsb.org/). The 3D-structure was processed with protein preparation wizard and hetero-molecules such as water and ligands were deleted from the protein. The H-atoms were appended including the protons

required for the proper ionization and generation of tautomeric states of charged amino acids viz., Asp, Ser, Glu, Arg and His. Further, it was energy minimized employing the OPLS-2005 force field to alleviate steric clashes (Teli and Rajanikant 2012).

In order to explore the binding ACE-2/spike binding domain, all the potential binding sites on the surface of the ACE-2/spike binding domain were probed. Binding sites were identified by means of SiteMap tool from Schrodinger (Halgren 2009). SiteMap identifies energetically potential binding site through a coordination of topological features computed at each site point employing van der Waals probes. SiteMap was lined up to predict the five top-ranked potential receptor sites using the default settings. The site score, druggability score and size were employed to ascertain the most favourable binding pocket.

Docking Based Screening Docking experiments were executed by employing Glide. The grid to set up the docking was created with standard parameters optimized for peptide docking. The grid box coordinates were centred at the site1 and the size of computed grid was based on the size of the peptides. Standard precision (SP) docking was employed in the docking based screening. To lighten the potential of nonpolar fragments of ligands, the scaling factor for the peptide van der Waals radii was adjusted to 1.0 with a partial atomic charge of 0.25. In the docking protocol, flexible peptide sampling was employed to construct diverse peptide conformations at pH of 7.0 ± 2.0. OPLS-3 force field was engaged to generate the state of peptides to rectify the structure, to minimize the conformations and generate protonation/tautomerization states of the peptides (Harder et al. 2016). No constraints were used in the entire docking studies. After docking, top-ranked peptides were compared with native peptides based on the GlideScore. Lower GlideScore with favourable hydrogen bond, hydrophobic and π interactions of the best poses were visualized and interpreted using maestro visualizer.

Molecular Dynamics (MD) Simulations

In order to investigate the stability and compatibility of top ranking docked peptides, MD simulations were implemented. Based on the docking based probing, two top scoring protein-peptide complexes were chosen to carry out the MD simulations using the GROMACS (Version-2020) (Van Der Spoel et al. 2005) and each protein-peptide complex was represented using the OPLS force field (Robertson et al. 2015). The complex was solvated by using single point charge (SPC) water model within a cubical measuring 1Å on each side. The ionic charge of the system was neutralized by adding inverse ions; overall a salt concentration of 0.15 M was maintained. The linear constraint (LINCS) algorithm

was applied to fix all hydrogen related bond lengths (Hess et al. 1997). Electrostatic interactions (long range) between atoms were managed by engaging Particle Mesh Ewald (PME), a cut-off of 1.0 nm was applied to both the PME direct-space constituent of electrostatic features and van der Waals interactions (Hess et al. 2008). The 3-stage system relaxation protocol was employed before the production simulation. This comprised of a sequence of minimization and equilibration runs to gradually relax the system while not ominously deviating from the primary conformation. The relaxation protocol employed are: (1) 50 ps energy minimization immediately after adding salt to the system, (2) Energy equilibration in NVT (constant number of particles, volume and temperature) ensemble at 300 K and (3) 100 ps MD simulation in NPT (constant number of particles, pressure and temperature) ensemble at 300 K. Finally, production simulations were executed in the NPT ensemble for 50 ns at 300 K temperature and 1.0 bar pressure. For this, the V-rescale (modified Berendsen thermostat) (Bussi et al. 2007) was applied with a time constant of 0.1 ps and the isotropic Parrinello-Rahman Barostat was used with a time constant of 2 ps (Berendsen et al. 1984). A cut off of 1.2 Å was used for assessing short-range van der Waals interactions. MD trajectories were saved by taking frames every 10 ps. After production simulations, root mean square deviations (RMSD), root mean square fluctuations (RMSF), and protein-peptide interactions of the complexes were ciphered.

Results and Discussion

Total protein was extracted from 500 g seeds of Buckwheat and Quinoa respectively and their yields were found to be 5 and 3.4% respectively. Statistical t and f test were performed and p value remained significant (P value < 0.0001).

In Vitro Gastrointestinal Digestion and Ultrafiltration

An in vitro digestion was performed in correlation to the realistic digestion of dietary proteins in the GI tract to unravel the cryptic peptides concealed within the proteins. The hydrolyzates were fractionated using MWCO of 3 kDa for enrichment of low molecular weight peptides and the permeates quantified for the peptide content varied from $7 \pm 0.13\%$ to $6 \pm 0.27\%$ for Buckwheat and Quinoa respectively.

Identification of Peptides by Nano-LC-MS/MS

A total of 21 peptides, 10 from pepsin digest and 11 from sequential digestion of pepsin & pancreatin ranging from 839.05 Da- LGIMVGHL to 2587.96

Da- GVKPVQSPGPFLAGMEPRYQSVSR for Buckwheat and a total of 13 peptides, 10 from pepsin digest and 3 from sequential digest of pepsin & pancreatin ranging from 930.14 - LVIPLGYR to 2368.61 Da-LQPRIVGNEHYETAQRVKET for Quinoa were identified and these sequences corresponded to 34 different proteins from the NCBInr data base search of Maize (Tables 1 and 2 respectively). To envisage preferential amino acids for potent antioxidant activity, the constituent amino acids among 34 peptides were analyzed and the result accounted for 40% antioxidant amino acids contributing for peptide solubility, conversion of free radicals to stable, effective metal ion chelating and for radical scavenging for protecting tissue from oxidative stress. Presence of antioxidant amino acids such as Leu, Tyr, Trp, Met, Phe, Pro, Ala, His, Lys, Val & Cys accounted for high antioxidant activity in both the Buckwheat and Quinoa permeates (Saidi et al. 2014).

Radical Scavenging Activity of Permeates

Permeates were assessed for antioxidant activity. Buckwheat permeate displayed IC_{50} at 108 ± 4 μg/ml and Quinoa permeate displayed IC_{50} at 128 ± 3 μg/ml. Majority of the antioxidative peptides were in the range of 3 to 16 amino acid residues and as reported earlier, the relationship between molecular weight and the antioxidant activity indicated that peptides below 1 kDa exhibited best antioxidant activities in ABTS and other radical scavenging assays (Ngoh and Gan 2016). ANOVA, Brown-Forsythe and Bartlett's statistical tests were performed and the p value statistically remained significant.

Gene Ontology Annotation, STRING 10 and Sub Cellular Localization Analysis

Functional annotation clustering in the default mode of all the identified proteins led to the clustering of the genes into 4 different gene functional groups, two each for Quinoa and Buckwheat (Fig. 1a and b). The 34 identified proteins participate in many pathways. On the basis of protein functions, these proteins were grouped into seven categories. Proteins like putative receptor protein kinase ZmPK1, Putative receptor protein kinase CRINKLY4, methylthioribose-1-phosphate isomerase and methionine S-methyltransferase participate in metabolism. Triosephosphate isomerase, cytosolic β-fructofuranosidase, glutamine synthetase root isozyme 2, bifunctional aspartokinase/homoserine dehydrogenase 1, chloroplastic, glutamate dehydrogenase, ATP synthase subunit beta, mitochondrial, ferredoxin-dependent glutamate synthase, chloroplastic, NAD(P)H-quinone oxidoreductase subunit 1, chloroplastic, sucrose synthase 1, ferredoxin-dependent glutamate synthase, chloroplastic, ATP synthase protein MI25, ATP synthase subunit beta, chloroplastic and

(S)-beta-macrocarpene synthase participate in energy pathways. Putative receptor protein kinase CRINKLY4, putative receptor protein kinase, pyruvate phosphate dikinase 1 and chloroplastic have signal transduction roles. Derlin, Preprotein translocase subunit SECY, chloroplastic, preprotein translocase subunit SECY and chloroplastic have protein destination and storage functions. DNA-directed RNA polymerase subunit β, autonomous transposable element EN-1 mosaic protein, CRS2-associated factor 1, chloroplastic and DNA (cytosine-5)-methyltransferase 1 have transcription regulation functions. Aquaporin TIP1-2 & aquaporin PIP1-1 have transportation function and finally Luminal-binding protein 2, homocysteine S-methyltransferase 1and Peroxidase 2 have defence functions.

With the above information, Gene Ontology (GO) analysis performed in the present study showed that in both Buckwheat and Quinoa, proteins related to metabolism and energy clustered together into one functionally related group with complete green 2D heat map showing highly common annotations. On the other hand, proteins related to signal transduction, protein destination and storage and transportation were clustered into one functionally related group with green-black map indicating the missing of few common annotations. Few of the identified proteins did not cluster into any functional annotation group as they were lacking other partners of common annotations.

Peptidomic data thus generated facilitated to explore protein-protein interaction using STRINGv10 in Buckwheat and Quinoa (Fig. 2a). For Buckwheat three association networks were identified. Out of three, one network was observed between proteins involved in transcription, transcription regulation and protein modelling, destination and storage. As the basis of this protein association network is the lines connecting proteins for functional relationship, co-expression, co-existence, gene fusion, proximity of genome and experimental & database evidence, imply that transcription & translation and their regulations are closely coupled. The other two associations were among proteins involved in energy and metabolism. For Quinoa single association network was observed involved in energy. Annotation and string analysis both revealed the same result, where in annotated proteins for similar annotation terms clustered into one and in string analysis also proteins involved in same or close biological process formed association network themselves showing associated proteins were functionally, experimentally and spatially related.

Further, sub-cellular localization of the identified proteins was predicted by wolf psort software (Fig. 2b). Among the identified proteins, 38% were localized in chloroplast, 22% cytoplasm, 18% plastids, 14% mitochondria and remaining one or two proteins were localized in extracellular, nucleus and endoplasmic reticulum. This localization indicates that the majority of the seed

Table 1 Bioactive peptide's primary structure (sequences), validation and identification by MS/MS analysis in Buckwheat

Ref. No[a]	Peptide SEq. & Res. fra. no[b]	Peptide mass[c]	Peptide threshold score[d]	% SPI[e]	Protein entry name & Accession no.[f]	Species for match & databas[g]
Pepsin Digest						
1	IAPASPQENL	1039.13	7.93	67.7	Putative receptor protein kinase CRINKLY4 O24585.1	MAIZE/NCBInr
2	LGIMVGHL	839.05	7.46	67.3	Derlin-1.2 Q4G2J5.1	MAIZE/NCBInr
3	LDIPQNNT	913.96	7.24	59.8	P16023.1 DNA-directed RNA polymerase subunit beta	MAIZE/NCBInr
4	LLARAAAAGXX	812.95	6.98	59.9	CASP-like protein 15 B6TWJ1.2	MAIZE/NCBInr
5	IAPAPRGTPQIEVTFEVDANG	2182.39	6.15	66.8	Luminal-binding protein 2 P24067.3	MAIZE/NCBInr
6	WKSTLRKSKPIYNRA	1848.16	5.21	58.2	Homocysteine S-methyltransferase 1 Q9FUN0.1	MAIZE/NCBInr
7	WNPDSAVWGNIT	1359.44	4.93	57	Beta-fructofuranosidase 1 P49175.1	MAIZE/NCBInr
8	FTGEVSAEMLVNLGVPWV	1948.24	4.73	69.5	Triosephosphate isomerase, cytosolic P12863.3	MAIZE/NCBInr
9	LKRQGASIPLVRPGKSTAAY	2113.47	4.34	65.8	Preprotein translocase subunit SECY, chloroplastic O63066.1	MAIZE/NCBInr
10	LSGPVDDPSKLPK	1352.53	4.22	56.2	Glutamine synthetase root isozyme 2 P38560.1	MAIZE/NCBInr
Pepsin and Pancreatin digest						
1	LAAPNNPSLR	1052.18	6.93	57.7	Peroxidase 2 Q9FEQ8.1	MAIZE/NCBInr
2	MAARNGVEPTLLQVFVEGHK	2196.53	6.52	50.6	Autonomous transposable element EN-1 mosaic protein P15268.1	MAIZE/NCBInr
3	IAVGAPGELSHPDTAK	1562.72	6.47	55.6	Aquaporin TIP1-2 Q9ATM0.1	MAIZE/NCBInr
4	FSERHAIGTAAQGTDDKDYK	2210.32	6.02	51.5	Aquaporin PIP1-1 Q41870.1	MAIZE/NCBInr
5	LTAFELVHEK	1186.35	5.95	55	Methylthioribose-1-phosphate isomerase B6TZD1.1	MAIZE/NCBInr
6	RQGASIPLVRPGKSTAAYIK	2113.47	5.47	67.4	Preprotein translocase subunit SECY, chloroplastic O63066.1	MAIZE/NCBInr
7	GVKPVQSPGPFLAGMEPRYQS-VSR	2587.96	5.33	79.1	CRS2-associated factor 1, chloroplastic Q84N49.1	MAIZE/NCBInr
8	NLYLEIQKKNLFASEMR	2097.44	5.16	80.4	DNA-directed RNA polymerase subunit beta'' P16025.1	MAIZE/NCBInr
9	FLSQLHADISNLKAMLR	1957.30	4.88	55.4	Bifunctional aspartokinase/homoserine dehydrogenase 1, chloroplastic P49079.1	MAIZE/NCBInr
10	ITEFFEGTDQCHYFTCR	2097.29	4.83	62.5	DNA (cytosine-5)-methyltransferase 1 Q9AXT8.1	MAIZE/NCBInr
11	MGAFTLGVNRVARATVLR	1932.30	4.35	53.4	Glutamate dehydrogenase Q43260.1	MAIZE/NCBInr

Table 1 (continued)

[a]Reference number for unique peptide sequence

[b]Peptide sequence and their residual numbers from its parental protein

[c]Peptide mass

[d]If a peptide sequence > 8 residues long was employed in identifying the corresponding protein, peptide threshold scores less than 6 seldom represent valid interpretations

[e]% scored peak intensity a measure of how much of your extracted spectrum is explained by the database result, must be greater than 60 to 90 in protein details mode and greater than 60 to 70 in peptide details mode

[f]Protein to which the peptide matches was observed along with their accession no

[g]Species for protein match: *MAIZE* & database: NCBI-nr

Table 2 Bioactive peptide's primary structure (sequences), validation and identification by MS/MS analysis in Quinoa

Ref. No[a]	Peptide SEq. & Res. fra. no[b]	Peptide mass[c]	Peptide threshold score[d]	% SPI[e]	Protein entry name & Accession no.[f]	Species for match & databas[g]
Pepsin Digest						
1	LSQPFHVAEVFTGAPGK	1783.91	8.05	55.4	ATP synthase subunit beta, mitochondrial P19023.1	MAIZE/NCBInr
2	LTLDELGRET	1146.24	8.01	60.7	Ferredoxin-dependent glutamate synthase, chloroplastic P23225.1	MAIZE/NCBInr
3	LVIPLGYR	930.14	7.51	70.5	NAD(P)H-quinone oxidoreductase subunit 1, chloroplastic P25706.3	MAIZE/NCBInr
4	FNIVSPGADMSV	1236.39	6.75	57.7	Sucrose synthase 1 P04712.1	MAIZE/NCBInr
5	LVLSDRSEAPEPTRPAIPI	2061.34	6.72	61.6	Ferredoxin-dependent glutamate synthase, chloroplastic P23225.1	MAIZE/NCBInr
6	FSGMDMKGINML	1343.63	5.82	62.1	ATP synthase protein MI25 P09004.1	MAIZE/NCBInr
7	LQPRIVGNEHYETAQRVKET	2368.61	5.49	54.5	ATP synthase subunit beta, chloroplastic P00827.1	MAIZE/NCBInr
8	LDSKLNRPVN	1155.30	5.09	60.5	Putative receptor protein kinase ZmPK1 P17801.2	MAIZE/NCBInr
9	IVEQKEELKNRANQL	1812.03	4.53	62.8	Methionine S-methyltransferase Q8W519.2	MAIZE/NCBInr
10	LAPLPIGFAVF	1144.40	4.37	54.4	Aquaporin PIP1-5 Q9AR14.1	MAIZE/NCBInr
Pepsin and Pancreatin digest						
1	FMIEQGLALKEYPIIVPR	2117.56	6.16	51.2	(S)-beta-macrocarpene synthase Q1EG72.1	MAIZE/NCBInr
2	NWRTVKYG	1023.14	5.86	59.6	Cell number regulator 4 D9HP20.1	MAIZE/NCBInr
3	AVVDAAPIQTTKKR	1497.73	5.63	52.4	Pyruvate, phosphate dikinase 1, chloroplastic 103585.5	MAIZE/NCBInr

[a]Reference number for unique peptide sequence

[b]Peptide sequence and their residual numbers from its parental protein

[c]Peptide mass

[d]If a peptide sequence > 8 residues long was employed in identifying the corresponding protein, peptide threshold scores less than 6 seldom represent valid interpretations.

[e]% scored peak intensity a measure of how much of your extracted spectrum is explained by the database result, must be greater than 60 to 90 in protein details mode and greater than 60 to 70 in peptide details mode

[f]Protein to which the peptide matches was observed along with their Accession No.

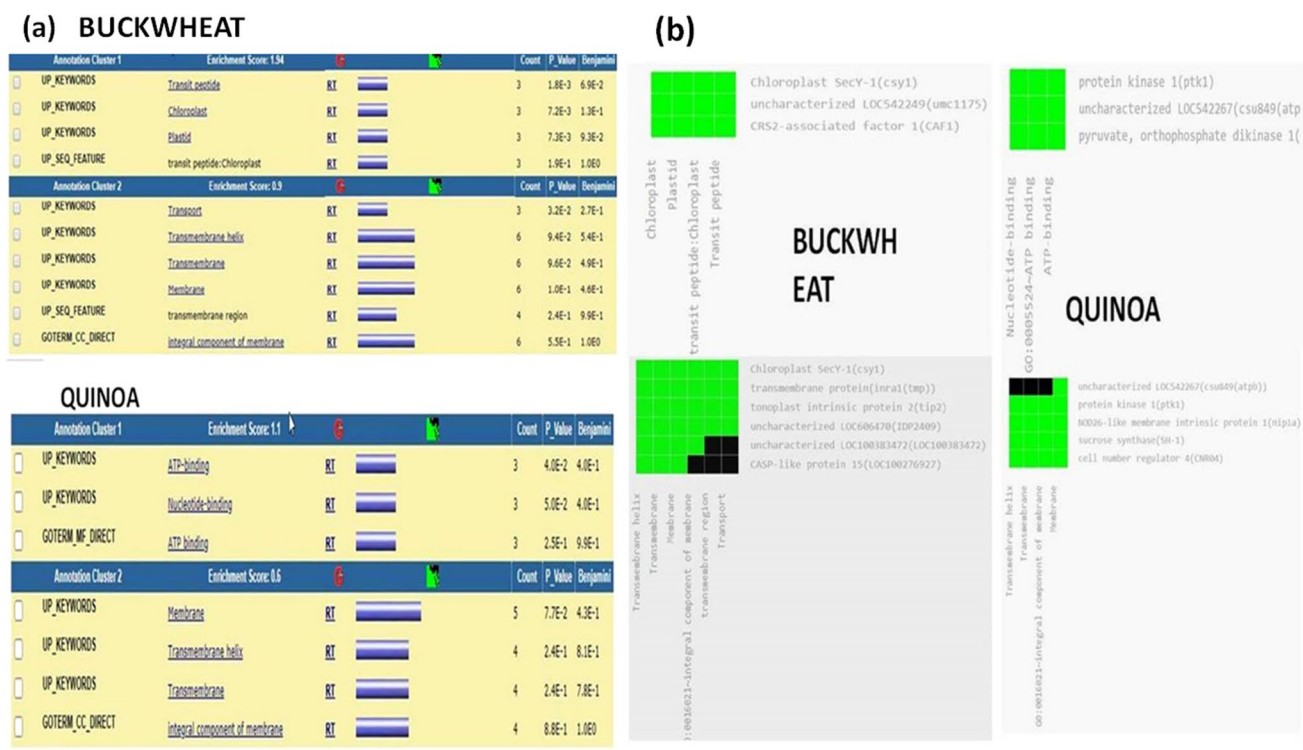[g]Species for protein match: *MAIZE* & database: NCBI-nr

Fig. 1 Functional Annotation Clustering of identified buckwheat and quinoa proteins was carried out in default settings. **a** Clustering of the genes into different gene functional groups were reported in a gene functional group clustering chart with (i) EASE Score (a modified Fisher Exact P-Value, for gene-enrichment analysis. It ranges from 0 to 1. Fisher Exact P-Value = 0 represents perfect enrichment. Usually P-Value is equal or smaller than 0.05 to be considered strongly enriched in the annotation categories. Default is 0.1) along with Benjamini (FDR corrected) p-value. (ii) Group Enrichment Score (It ranks the biological significance of gene groups based on overall EASE scores of all enriched annotation terms of that corresponding gene group, Thus, the top ranked annotation groups most likely have consistent lower p-values for their annotation members). **b** Gene members clustered into different gene functional groups (2 clusters each for buckwheat and quinoa respectively) and their associated annotation term on 2-D heatmap type view allowed to examine the common and difference of annotations cross the group gene members (gene-gene and term-term relationships within a group). Each gene cluster was viewed on a separate 2-D heatmap with genes in a corresponding gene functional group listed vertically and annotation terms horizontally. On a 2-D heatmap green area shows highly common of annotations and black-green area shows difference of annotations (Color figure online)

proteins are involved in energy production in chloroplast and mitochondria and the produced energy was transported via cytoplasm and stored in plastids. Recently, a comprehensive shot-gun proteomics approach was applied by Wang and colleagues (Wang et al. 2019) to identify several seed proteins of tartary Buckwheat using Trypsin. In the same study, the major distribution profile of subcellular localization of identified proteins indicated 39.9% in chloroplast, 25.1% in cytoplasm, 16.2% nucleus and 6.4% in mitochondria as well as the GO annotation analysis was in accordance with our study. A similar shot-gun proteomic approach was also used to identify 16 storage proteins from different Quinoa seed genotypes through TCA/Acetone protein extraction, using label-free shotgun proteomics followed by in silico analysis, with the three published Quinoa genomes (Burrieza et al. 2019). Among the sixteen globulins, thirteen were novel, nine legumin-like proteins and seven vicilin-like proteins. Seven of the novel proteins were found to contain 7.5% or more of lysine mass, justifying the high content of lysine frequently reported in Quinoa seeds.

Investigation of Bioactivity Profiles of Generated Peptides Using BIOPEP Database

Few studies have identified peptides from bioactive fractions of Buckwheat and Quinoa (Li et al. 2002; Ma et al. 2006; Rizzello et al. 2017; Obaroakpo et al. 2019; Luo et al. 2020). Hence, the bioactive profile of peptides derived from Buckwheat and Quinoa were investigated using the database-based search tool-BIOPEP. The data derived from BIOPEP analysis was represented in the form of pie-charts in Fig. 3a and b. A total of 463 peptides with 19 different reported bioactivities were found to match with the peptide sequences derived from Buckwheat, while, 239 peptides with 18 varied bioactivities matched with peptide sequences
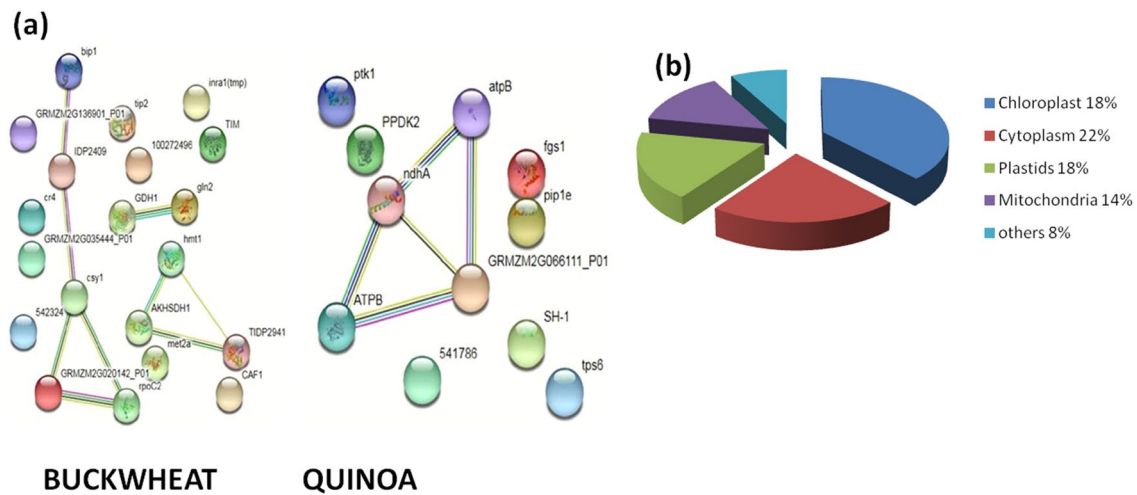
Fig. 2 **a** Association network among the identified buckwheat and quinoa proteins as predicted by STRING software against *Zea Mays*. The node represents the differentially accumulated protein while the different colored edges represent different evidences for the predicted functional relationship between proteins: green line—neighborhood genome evidence; red line—gene fusion evidence; dark blue line— co-occurrence evidence; pink line—experimental evidence; light blue line—database evidence; black line—co expression evidence; and yellow line—text-mining evidence. STRING IDs and the abbreviations of these interacting proteins along with their predicted functional partners. **b** Prediction of localization of proteins (Color figure online)
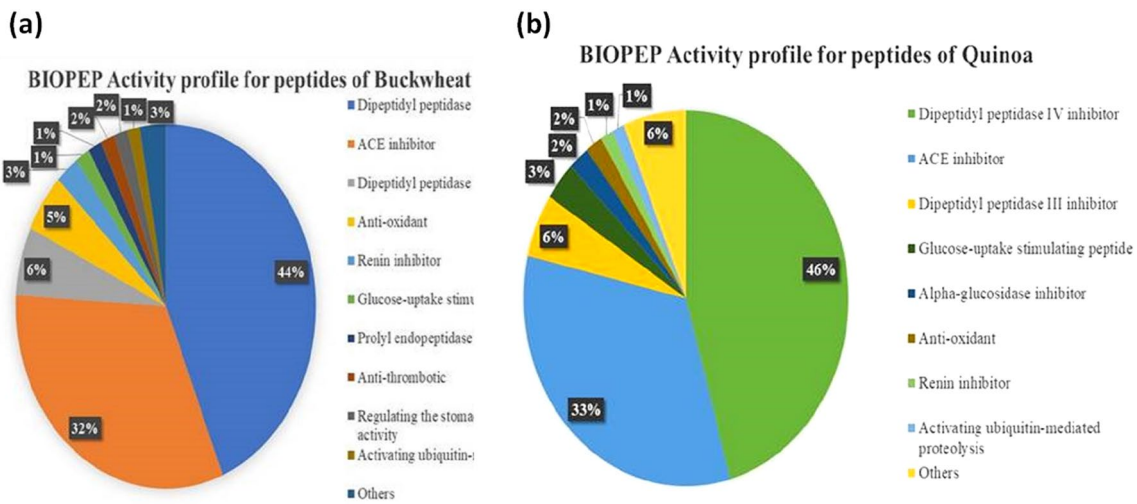

Fig. 3 **a** The summary of bioactivity profile for peptides derived from in vitro gastrointestinal simulation digestion of Buckwheat proteins; **b** The summary of bioactivity profile for peptides derived from in vitro gastrointestinal simulation digestion of Quinoa proteins

derived from Quinoa. Interestingly, peptides from both the millets displayed higher degree of Dipeptidyl peptidase IV and ACE-inhibitions (Supplementary). With the BIOPEP analyses it is evident that peptides derived from Buckwheat and Quinoa lack the comprehensive investigation bestowed to other sources such as milk and dairy based products.

The bioactivity profile generated through BIOPEP as mentioned earlier relies on reports of already published peptides for the particular bioactivity. Hence, emphasizing that most of these activities have been extensively explored in other sources of food proteins. In the present study the protein hydrolysates of both Buckwheat and Quinoa exhibited anti-oxidant activities in vitro. Notably, in both Buckwheat and Quinoa, the peptide sequences with anti-oxidant accounted for 5 and 1% respectively among the total bioactivities. Given their rich nutritional profile, protein content, the reported health benefits, and the in silico bioactivity profile, we opined that both Buckwheat

and Quinoa have excellent potential to be investigated for novel bioactivities against newer targets.

Prediction of Probable Binding Sites in ACE-2

SiteMap is an energetic grid-based method, which affiliates site druggability with binding affinity of ligand molecules (Halgren 2009). The SiteMap identified five potential binding sites in the ACE-2 domain. We selected the putative site that spanned the ACE-2-Spike binding domain. Further, the SiteMap disclosed the pharmaco features, namely H-bond acceptor, H-bond donor, hydrophilic, hydrophobic and metal binding sites. The H-bond donor and hydrophilic areas covered the maximal expanse of this binding pocket. The site was composed of nearly 15 residues (Fig. 4a and b).

Molecular Docking

To study the molecular basis of interactions and affinities, the library of peptides were formed and employed in a molecular docking study employing the glide docking module. The binding modes of all the peptides were ranked based on the docking score and their ability to fulfil the pre-defined constraints. The docking results of the screened peptides are depicted in Table 3. Out of the 35 docked complexes generated, the top 10 potential hits were selected by visual inspection, Glide Score and E-model score, to study their interactions with the binding site residues (Friesner et al. 2006). The 3-D molecular interactions of the identified ligands are displayed in Fig. 4a. The top four peptides were then obtained and evaluated for postdocking analysis, as well as their selectivity to the ACE-2 protein (Fig. 5).

Based on our docking experiments, we selected NWRT-VKYG as a potential inhibitor of ACE-2/spike with a docking score of −12.43 with and the corresponding E-model value was −213.63. Molecular docking analysis of four potential peptides showed that they shared a common intermolecular interaction with the protein. All of them were able to form H-bonds with Asp206 and Lys562. Examination of
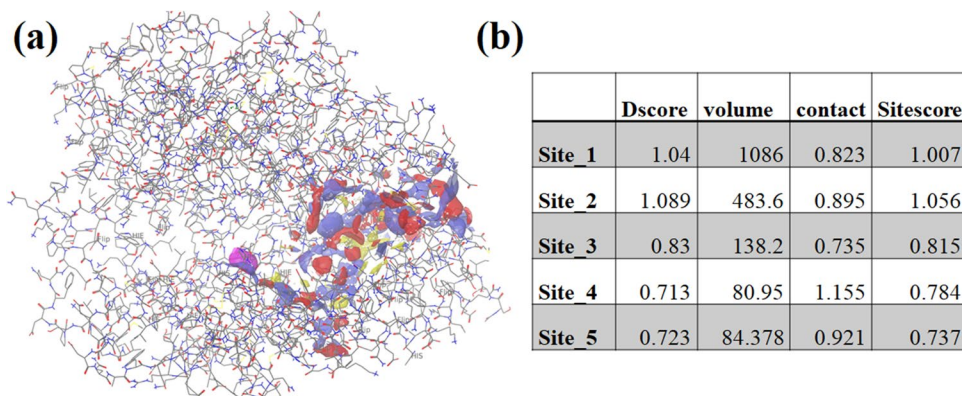
the binding modes of the peptides revealed that NWRT-VKYG adopted the classic binding mode of the C-end peptide, in which Tyr7 at the C-terminal formed H-bond with two key residues viz. Glu102 and Asn394. Lys6 exhibited 2 H-bond interactions with Asp206, Glu398 and one salt-bridge with Asp206. At the NH -terminal of the peptide, Asn1 formed a single H-bond with Glu208 and a network H-bonds were observed between remaining residues of the peptide-2 except Gly8 (Table 4).

Even though LAPLPIGFAVF had highest docking score of −13.47 and binding energy of −213.86 kcal/mol, and showed strong hydrophobic interactions but owing to its poor physicochemical properties and minimal interactive conformations led to the selection of NWRTVKYG which presented favourable interactions at every conformation. In the light of the docking scores, hydrogen bond, binding energy and physicochemical properties we opined that peptide-2 to be potential ACE-2 inhibitor and the same was validated by Molecular dynamic simulation studies.

Molecular Dynamic Simulation

We created two different systems of protein and subjected each one of them to 50 ns MD simulations. To evaluate the stability of the protein-peptide composite, we analyzed the root mean square deviation (RMSD) of the backbone atoms of protein in comparison to the minimized protein as a function of the simulation time. RMSD is an indispensable parameter which can be employed to envision the equilibration of system during the simulation (Sargsyan et al. 2017). In correspondence with our expectations, the native form of the protein showed slightly larger structural deviations which in average were 0.37 Å (Fig. 6a), which indicates that the unbound form of ACE-2 is slightly unstable in physiological conditions. On the other hand, the peptide-bound proteins exhibited a global variation of less than 0.23 Å, portraying their greater structural stability in inhibitor-bound states. Further, we observed that the both native and peptide-bound

Fig. 4 **a** Predicted binding site (sitemap1) on the surface of the ACE-2protein. **b** Potential binding sites identified in the modeled ACE-2 protein
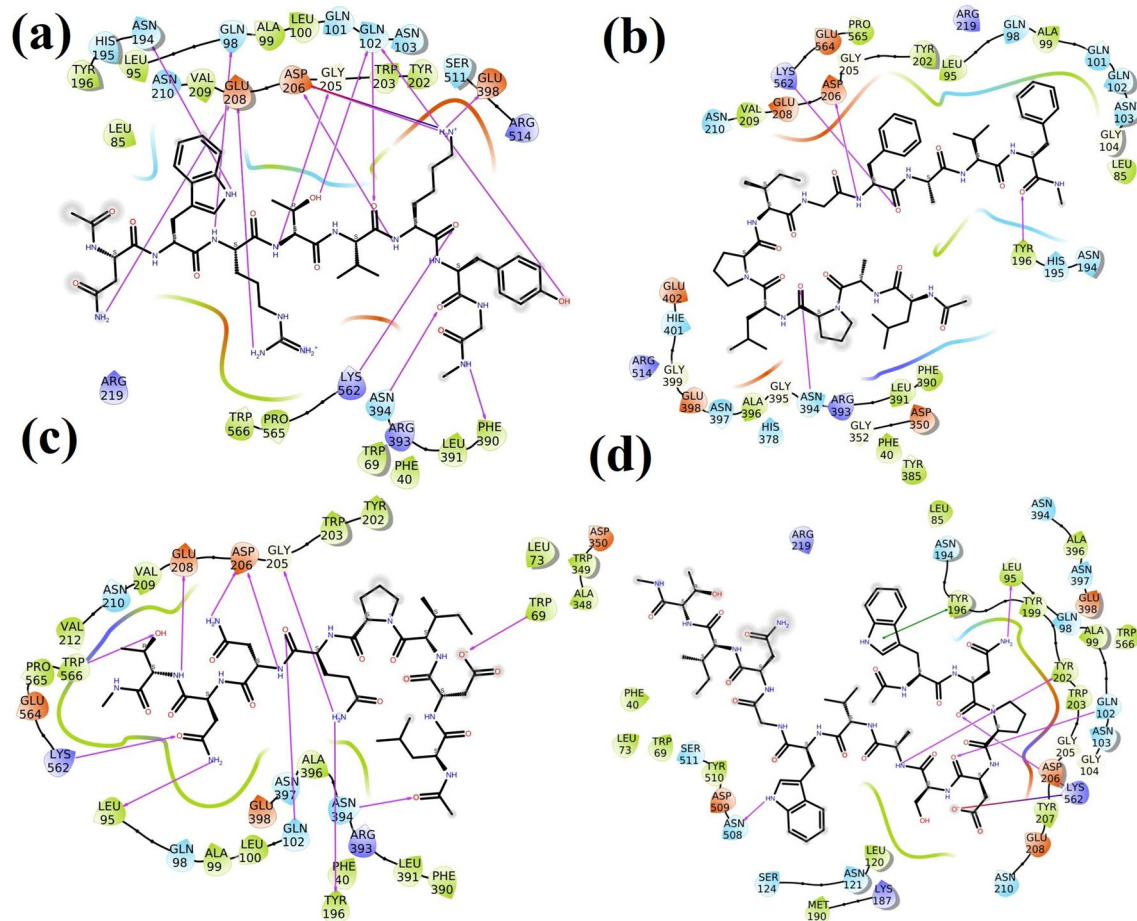
	Dscore	volume	contact	Sitescore
Site_1	1.04	1086	0.823	1.007
Site_2	1.089	483.6	0.895	1.056
Site_3	0.83	138.2	0.735	0.815
Site_4	0.713	80.95	1.155	0.784
Site_5	0.723	84.378	0.921	0.737

Fig. 5 "Top scored peptides" docked into the Site1 of *ACE-2*: Depicting the amino acids of the target protein interacting with the ligands

Table 3 Glide Protein-Peptide docking results of the potential peptides

Title	H-bond	Evdw	Ecoul	Emodel	Glide score
LAPLPIG-FAVF	−0.76	−102.13	−22.77	−213.56	−13.47
NWRTVKYG	−2.27	−68.33	−50.59	−213.63	−12.43
LDIPQNNT	−1.84	−64.64	−26.6	−152.12	−12.34
WNPDSAVW-GNIT	−1.62	−82.86	−20.73	−167.87	−12.08
LDSKLNR-PVN	−2.12	−70.62	−34.16	−195.82	−11.37
LTAFELVHEK	−1.08	−73.22	−30.08	−180.85	−11.09
FSGMDMK-GINML	−1.57	−71.95	−27.40	−156.05	−10.32
LLARAAAAG	−1.98	−58.82	−27.06	−152.14	−10.22
IAPASPQENL	−1.41	−66.90	−17.10	−117.27	−10.19
LVIPLGYR	−0.49	−63.58	−22.29	−132.87	−10.16
IAPASPQENL	−1.82	−61.02	−24.61	−129.98	−10.13

Table 4 Interaction Profile of the NWRTVKYG

NWRTVKYG	
Asn1 : Glu208	NH2…OH
Trp2 : Asn194	NH2…C=O
Arg3 : Gln98	NH2…C=O
Arg3 : Gln208	NH2…C=O
Thr4 : Gly205	NH2…C=O
Thr4 : Gln102	OH…C=O
Val5 : Gln102	C=O…NH2
Lys6 : Asp206	N…OH (Salt Bridge)
Lys6 : Glu398	NH2…C=O
Lys6 : Asp206	NH2…C=O
Lys6 : Asp206	NH2…C=O
Tyr7 : Gln102	OH…C=O
Tyr7 : Asn394	C=O…NH2
Tyr7 : Phe390	C=O…NH2

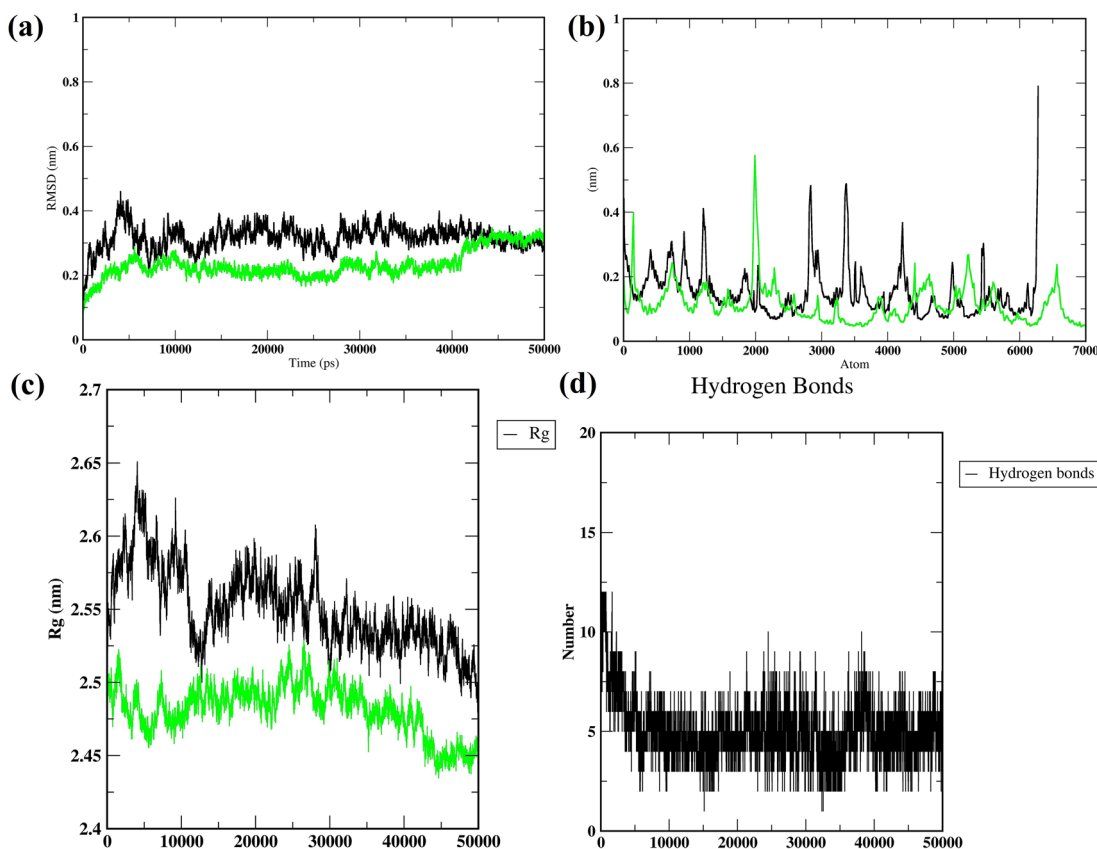complexes reached an equilibrated state after 12 and 10 ns respectively.

Fig. 6 Molecular dynamics simulation results: **a** The comparison of root mean square deviation (RMSD) values of backbone atoms for the native and ACE-2-Peptide complex. **b** RMS fluctuation curves obtained from molecular dynamics simulation for the native and ACE-2-Peptide complex. **c** Radius of gyrations for the native and ACE-2-Peptide complex. **d** Hydrogen bonding patterns during the course of simulations for the native and ACE-2-Peptide complex

The RMSF is a great tool that delivers a superior understanding of the flexibility and fluctuations of the protein structure (Dong et al. 2018). To probe the flexibility of the ACE-2, we computed the RMSF value for both ACE-2, ACE-2- Peptide during the course of the simulation. The RMSF value of the aforesaid protein systems is illustrated in Fig. 6b. As depicted, the ACE-2 has the least flexibility of the residues at the binding site in presence of peptide. The conclusion that can be drawn by these observations is that the predicted inhibitor has a close interaction with the binding site of ACE-2, thus lowering the fluctuation of the ACE-2. Similar to RMSD, the Radius of gyration (Rg) discloses the stability of the equilibrated protein and compactness of the protein during simulation (Lobanov et al. 2008). In the present study, it was observed that the Rg results indicated better compactness of peptide-bound complex compared to native protein. These results clearly indicate the stability brought about by the structural modifications imparted by the bound peptide (Fig. 6c).

To probe the binding site residues involved in H-bond formation and inhibitor recognition, H-bond occupancies

were computed. The number of hydrogen bonds varied during simulation and the average H-bond occupancy was 8 (Fig. 6d). Further, it can be ascertained that Gln102, Asp206 and Glu208 were major residues involved in H-bond interactions and other amino acids that form polar interactions and responsible for peptide recognition were Gln98, Asn194, Gly205 and Lys562 with the ACE-2 system. The H-bond analysis confirms the significance of polar interactions in the selective recognition of agonist and antagonist molecules. Finally, the RMSD, Rg, RMSF and H-Bond results corroborate the structural stability of the protein in presence of peptide inhibitor.

At present, ACE-2 is regarded as the functional receptor for spike proteins of SARS-CoV (Li et al. 2003; Xiao et al. 2003), and also believed to serve as a functional human receptor for SARS-CoV2, responsible for the current COVID-19 pandemic (Sharifkashani et al. 2020; Wan et al. 2020). SARS-CoV spike protein is known to have strong binding affinity to human ACE-2. Further, SARS- CoV-2 and SARS-CoV spike proteins share 76.5% identity in their amino acid sequences (Xu et al. 2020b) and homology (Xu

et al. 2020b). Additionally, research even suggests that SARS-CoV-2 recognizes human ACE-2 more efficiently than SARS-CoV thereby increasing the ability of SARS-CoV-2 to transmit from person to person (Wan et al. 2020). Zhang et al. (2020) recently reviewed the molecular mechanisms for potential therapeutic targets to combat COVID-19, which involve (i) Spike protein-based vaccine, (ii) Inhibition of transmembrane protease serine 2 (TMPRSS2) activity, (iii) Blocking ACE-2 receptor and (iv) Delivering excessive soluble form of ACE-2. While the tedious hunt for vaccine continues, use of virtual screening high throughput techniques for small molecule inhibitors offer a quicker alternative strategy to block the interactions between ACE-2 receptor and Spike protein of SARS-CoV-2 (Chen et al. 2020; Zhang et al. 2020). In a recent study (Wu et al. 2020), natural compounds and the ZINC database was used to screen potential therapeutic targets for SARS-CoV-2. Among the targets, most of the compounds chosen were not predicted to bind with the binding interface of the Spike-ACE-2 complex with the exception of hesperidin. ACE-2 receptor as mentioned earlier, is known to be highly expressed on the mucosa of oral cavity, especially enriched in the epithelial cells of the tongue (Xu et al. 2020a). Hence, bioactive peptides derived from Buckwheat and Quinoa was screened against ACE-2 and one of the lead peptide exhibited promising results as a potential therapeutic agent.

Conclusions

The present study aided in identification and characterization of Buckwheat and Quinoa proteins after in vitro gastrointestinal simulation digestion. The proteomic analysis in the present study also clearly ascertained and established how the seed proteome works, i.e., proteins from dietary seeds work together functionally and spatially in the expression & regulation of genes involved in the production of energy, energy production in chloroplast & mitochondria, energy transport through cytoplasm and storage of this energy food in plastids and vacuoles, a clear functional outlook of what proteome from seeds should do. In addition, the peptides identified served as a library for exploring the potential bioactivities encrypted within the proteins through the computational database by BIOPEP bioactivity profiling. Although the peptides displayed an array of bioactivities, the present study explored peptides which can bind to ACE-2 target of Spike protein of the SARS-CoV-2 through molecular docking and dynamics due to its current prominence. Of the 11 potential peptides that interacted with ACE-2, the peptide NWRTVKYG from Quinoa was found to be most effective in silico. Therefore, production and processing of peptides

based on important structure-function parameters can lead to the production of potent SARS-CoV-2 peptide inhibitor/s.

Declarations

Conflict of interest The authors declare no competing interests.

Consent to publish All authors provided final approval for the publication of the paper.

References

Abugoch James LE (2009) Quinoa (*Chenopodium quinoa* Willd.): composition, chemistry, nutritional, and functional properties. Adv Food Nutr Res 58:1–31. https://doi.org/10.1016/S1043-4526(09)58001-1

Admassu H, Gasmalla MAA, Yang R, Zhao W (2018) Identification of bioactive peptides with α-amylase inhibitory potential from enzymatic protein hydrolysates of red seaweed (*Porphyra* spp). J Agric Food Chem 66:4872–4882. https://doi.org/10.1021/acs.jafc.8b00960

Aluko RE, Monu E (2003) Functional and bioactive properties of quinoa seed protein hydrolysates. J Food Sci 68:1254–1258. https://doi.org/10.1111/j.1365-2621.2003.tb09635.x

Ashok NR, Aparna HS (2017) Empirical and bioinformatic characterization of buffalo (*Bubalus bubalis*) colostrum whey peptides & their angiotensin I-converting enzyme inhibition. Food Chem 228:582–594. https://doi.org/10.1016/j.foodchem.2017.02.032

Benjamini Y, Hochberg Y (1995) Controlling the false discovery rate: a practical and powerful approach to multiple testing. J R Stat Soc Ser B 57:289–300. https://doi.org/10.1111/j.2517-6161.1995.tb02031.x

Berendsen HJC, Postma JPM, Van Gunsteren WF et al (1984) Molecular dynamics with coupling to an external bath. J Chem Phys 81:3684–3690. https://doi.org/10.1063/1.448118

Bhat ZF, Kumar S, Bhat HF (2017) Antihypertensive peptides of animal origin: a review. Crit Rev Food Sci Nutr 57:566–578. https://doi.org/10.1080/10408398.2014.898241

Burrieza HP, Rizzo AJ, Moura Vale E et al (2019) Shotgun proteomic analysis of quinoa seeds reveals novel lysine-rich seed storage globulins. Food Chem 293:299–306. https://doi.org/10.1016/j.foodchem.2019.04.098

Bussi G, Donadio D, Parrinello M (2007) Canonical sampling through velocity rescaling. J Chem Phys 10(1063/1):2408420

Chakrabarti S, Guha S, Majumder K (2018) Food-derived bioactive peptides in human health: challenges and opportunities. Nutrients 10:1738. https://doi.org/10.3390/nu10111738

Chalamaiah M, Yu W, Wu J (2018) Immunomodulatory and anticancer protein hydrolysates (peptides) from food proteins: a review. Food Chem 245:205–222

Chalamaiah M, Keskin Ulug S, Hong H, Wu J (2019) Regulatory requirements of bioactive peptides (protein hydrolysates) from

food proteins. J Funct Foods 58:123–129. https://doi.org/10.1016/j.jff.2019.04.050

Chen Y, Guo Y, Pan Y, Zhao ZJ (2020) Structure analysis of the receptor binding of 2019-nCoV. Biochem Biophys Res Commun 525:135–140. https://doi.org/10.1016/j.bbrc.2020.02.071

Church FC, Swaisgood HE, Porter DH, Catignani GL (1983) Spectrophotometric assay using o-phthaldialdehyde for determination of proteolysis in milk and isolated milk proteins. J Dairy Sci 66:1219–1227. https://doi.org/10.3168/jds.S0022-0302(83)81926-2

Ciudad-Mulero M, Fernández-Ruiz V, Matallana-González MC, Morales P (2019) Dietary fiber sources and human benefits: the case study of cereal and pseudocereals. Advances in food and nutrition research. Academic Press Inc., Cambridge, pp 83–134

Comai S, Bertazzo A, Bailoni L et al (2007) The content of proteic and nonproteic (free and protein-bound) tryptophan in quinoa and cereal flours. Food Chem 100:1350–1355. https://doi.org/10.1016/j.foodchem.2005.10.072

Díaz-Gómez JL, Castorena-Torres F, Preciado-Ortiz RE, García-Lara S (2017) Anti-cancer activity of maize bioactive peptides. Front Chem 5:44. https://doi.org/10.1073/pnas.1718910115

Dong YW, Liao ML, Meng XL, Somero GN (2018) Structural flexibility and protein adaptation to temperature: molecular dynamics analysis of malate dehydrogenases of marine molluscs. Proc Natl Acad Sci USA 115:1274–1279. https://doi.org/10.1073/pnas.1718910115

Food and Agriculture Organization of the United Nations (2018) FAOSTAT statistical database. FAO, Rome

Friesner RA, Murphy RB, Repasky MP et al (2006) Extra precision glide: docking and scoring incorporating a model of hydrophobic enclosure for protein-ligand complexes. J Med Chem 49:6177–6196. https://doi.org/10.1021/jm051256o

Halgren TA (2009) Identifying and characterizing binding sites and assessing druggability. J Chem Inf Model 49:377–389. https://doi.org/10.1021/ci800324m

Harder E, Damm W, Maple J et al (2016) OPLS3: a force field providing broad coverage of drug-like small molecules and proteins. J Chem Theory Comput 12:281–296. https://doi.org/10.1021/acs.jctc.5b00864

Hernández-Ledesma B (2019) Quinoa (*Chenopodium quinoa* Willd.) as source of bioactive compounds: a review. Bioact Compd Heal Dis 2:27. https://doi.org/10.31989/bchd.v2i3.556

Hess B, Bekker H, Berendsen HJC, Fraaije JGEM (1997) LINCS: a linear constraint solver for molecular simulations. J Comput Chem 18:1463–1472

Hess B, Kutzner C, Van Der Spoel D, Lindahl E (2008) GRGMACS 4: algorithms for highly efficient, load-balanced, and scalable molecular simulation. J Chem Theory Comput 4:435–447. https://doi.org/10.1021/ct700301q

Hou C, Wu L, Wang Z et al (2019) Purification and identification of antioxidant alcalase-derived peptides from sheep plasma proteins. Antioxidants. https://doi.org/10.3390/antiox8120592

Ji X, Han L, Liu F et al (2019) A mini-review of isolation, chemical properties and bioactivities of polysaccharides from buckwheat (*Fagopyrum* Mill). Int J Biol Macromol 127:204–209

Lafarga T, Hayes M (2017) Bioactive protein hydrolysates in the functional food ingredient industry: overcoming currentchallenges. Food Rev Int 33:217–246. https://doi.org/10.1080/87559129.2016.1175013

Li CH, Matsui T, Matsumoto K et al (2002) Latent production of angiotensin I-converting enzyme inhibitors from buckwheat protein. J Pept Sci 8:267–274. https://doi.org/10.1002/psc.387

Li W, Moore MJ, Vasllieva N et al (2003) Angiotensin-converting enzyme 2 is a functional receptor for the SARS coronavirus. Nature 426:450–454. https://doi.org/10.1038/nature02145

Li S, Liu L, He G, Wu J (2018) Molecular targets and mechanisms of bioactive peptides against metabolic syndromes. Food Funct 9:42–52. https://doi.org/10.1039/c7fo01323j

Li X, Da S, Li C et al (2018) Effects of high-intensity ultrasound pretreatment with different levels of power output on the antioxidant properties of alcalase hydrolyzates from Quinoa (*Chenopodium quinoa* Willd.) protein isolate. Cereal Chem 95:518–526. https://doi.org/10.1002/cche.10055

Li-Chan ECY (2015) Bioactive peptides and protein hydrolysates: research trends and challenges for application as nutraceuticals and functional food ingredients. Curr Opin Food Sci 1:28–37. https://doi.org/10.1016/j.cofs.2014.09.005

Lobanov MY, Bogatyreva NS, Galzitskaya OV (2008) Radius of gyration as an indicator of protein structure compactness. Mol Biol 42:623–628. https://doi.org/10.1134/S0026893308040195

Luo X, Fei Y, Xu Q et al (2020) Isolation and identification of antioxidant peptides from tartary buckwheat albumin (*Fagopyrum tataricum* Gaertn.) and their antioxidant activities. J Food Sci 85:611–617. https://doi.org/10.1111/1750-3841.15004

Ma MS, In YB, Hyeon GL, Yang CB (2006) Purification and identification of angiotensin I-converting enzyme inhibitory peptide from buckwheat (*Fagopyrum esculentum* Moench). Food Chem 96:36–42. https://doi.org/10.1016/j.foodchem.2005.01.052

Meram C, Wu J (2017) Anti-inflammatory effects of egg yolk livetins (α, β, and γ-livetin) fraction and its enzymatic hydrolysates in lipopolysaccharide-induced RAW 264.7 macrophages. Food Res Int 100:449–459. https://doi.org/10.1016/j.foodres.2017.07.032

Mohanty D, Jena R, Choudhury PK et al (2016) Milk derived antimicrobial bioactive peptides: a review. Int J Food Prop 19:837–846. https://doi.org/10.1080/10942912.2015.1048356

Monteil V, Kwon H, Prado P et al (2020) Inhibition of SARS-CoV-2 infections in engineered human tissues using clinical-grade soluble human ACE2. Cell 181:905-913.e7. https://doi.org/10.1016/j.cell.2020.04.004

Morales D, Miguel M, Garcés-Rimón M (2020) Pseudocereals: a novel source of biologically active peptides. Crit Rev Food Sci Nutr. https://doi.org/10.1080/10408398.2020.1761774

Nagaoka S (2019) Structure–function properties of hypolipidemic peptides. J Food Biochem 43:e12539. https://doi.org/10.1111/jfbc.12539

Nakai K, Horton P (1999) PSORT: a program for detecting sorting signals in proteins and predicting their subcellular localization. Trends Biochem Sci 24:34–35. https://doi.org/10.1016/S0968-0004(98)01336-X

Nascimento AC, Mota C, Coelho I et al (2014) Characterisation of nutrient profile of quinoa (Chenopodium quinoa), amaranth (*Amaranthus caudatus*), and purple corn (*Zea mays* L.) consumed in the North of Argentina: proximates, minerals and trace elements. Food Chem 148:420–426. https://doi.org/10.1016/j.foodchem.2013.09.155

Navruz-Varli S, Sanlier N (2016) Nutritional and health benefits of quinoa (*Chenopodium quinoa* Willd.). J Cereal Sci 69:371–376

Ngoh YY, Gan CY (2016) Enzyme-assisted extraction and identification of antioxidative and α-amylase inhibitory peptides from Pinto beans (*Phaseolus vulgaris* cv. Pinto). Food Chem 190:331–337. https://doi.org/10.1016/j.foodchem.2015.05.120

Nielsen TB, Reynolds JA (1978) Measurements of molecular weights by gel electrophoresis. Methods Enzymol 48:3–10. https://doi.org/10.1016/S0076-6879(78)48003-6

Nongonierma AB, FitzGerald RJ (2018) Enhancing bioactive peptide release and identification using targeted enzymatic hydrolysis of milk proteins. Anal Bioanal Chem 410:3407–3423. https://doi.org/10.1007/s00216-017-0793-9

Nongonierma AB, Le Maux S, Dubrulle C et al (2015) Quinoa (*Chenopodium quinoa* Willd.) protein hydrolysates with in vitro

dipeptidyl peptidase IV (DPP-IV) inhibitory and antioxidant properties. J Cereal Sci 65:112–118. https://doi.org/10.1016/j.jcs.2015.07.004

Obaroakpo JU, Liu L, Zhang S et al (2019) α-Glucosidase and ACE dual inhibitory protein hydrolysates and peptide fractions of sprouted quinoa yoghurt beverages inoculated with *Lactobacillus casei*. Food Chem. https://doi.org/10.1016/j.foodchem.2019.1249852019.124985

Re R, Pellegrini N, Proteggente A et al (1999) Antioxidant activity applying an improved ABTS radical cation decolorization assay. Free Radic Biol Med 26:1231–1237. https://doi.org/10.1016/S0891-5849(98)00315-3

Rizzello CG, Tagliazucchi D, Babini E et al (2016) Bioactive peptides from vegetable food matrices: research trends and novel biotechnologies for synthesis and recovery. J Funct Foods 27:549–569. https://doi.org/10.1016/j.jff.2016.09.023

Rizzello CG, Lorusso A, Russo V et al (2017) Improving the antioxidant properties of quinoa flour through fermentation with selected autochthonous lactic acid bacteria. Int J Food Microbiol 241:252–261. https://doi.org/10.1016/j.ijfoodmicro.2016.10.035

Robertson MJ, Tirado-Rives J, Jorgensen WL (2015) Improved peptide and protein torsional energetics with the OPLS-AA force field. J Chem Theory Comput 11:3499–3509. https://doi.org/10.1021/acs.jctc.5b00356

Ruales J, de Grijalva Y, Lopez-Jaramillo P, Nair BM (2002) The nutritional quality of an infant food from quinoa and its effect on the plasma level of insulin-like growth factor-1 (IGF-1) in undernourished children. Int J Food Sci Nutr 53:143–154. https://doi.org/10.1080/09637480220132157

Ruan J, Zhou Y, Yan J et al (2020) Tartary buckwheat: an under-utilized edible and medicinal herb for food and nutritional security. Food Rev Int. https://doi.org/10.1080/87559129.2020.1734610

Saidi S, Deratani A, Belleville MP, Ben Amar R (2014) Antioxidant properties of peptide fractions from tuna dark muscle protein by-product hydrolysate produced by membrane fractionation process. Food Res Int 65:329–336. https://doi.org/10.1016/j.foodres.2014.09.023

Santos RAS, Ferreira AJ, Verano-Braga T, Bader M (2013) Angiotensin-converting enzyme 2, angiotensin-(1–7) and Mas: new players of the renin-angiotensin system. J Endocrinol. https://doi.org/10.1530/JOE-12-0341

Sargsyan K, Grauffel C, Lim C (2017) How molecular size impacts RMSD applications in molecular dynamics simulations. J Chem Theory Comput 13:1518–1524. https://doi.org/10.1021/acs.jctc.7b00028

Schoenlechner R, Siebenhandl S, Berghofer E (2008) Pseudocereals. Gluten-free cereal products and beverages. Elsevier Inc., Amsterdam, pp 149–190

Sharifkashani S, Bafrani MA, Khaboushan AS et al (2020) Angiotensin-converting enzyme 2 (ACE2) receptor and SARS-CoV-2: potential therapeutic targeting. Eur J Pharmacol 884:173455. https://doi.org/10.1016/j.ejphar.2020.173455

Takao T, Watanabe N, Yuhara K et al (2005) Hypocholesterolemic effect of protein isolated from quinoa (*Chenopodium quinoa* willd.) seeds. Food Sci Technol Res 11:161–167. https://doi.org/10.3136/fstr.11.161

Teli MK, Rajanikant GK (2012) Pharmacophore generation and atom-based 3D-QSAR of N-iso-propyl pyrrole-based derivatives as HMG-CoA reductase inhibitors. Org Med Chem Lett 2:25. https://doi.org/10.1186/2191-2858-2-25

Tsai JS, Chen TJ, Pan BS et al (2008) Antihypertensive effect of bioactive peptides produced by protease-facilitated lactic acid fermentation of milk. Food Chem 106:552–558. https://doi.org/10.1016/j.foodchem.2007.06.039

Van Der Spoel D, Lindahl E, Hess B et al (2005) GROMACS: fast, flexible, and free. J Comput Chem 26:1701–1718

Vega-Gálvez A, Miranda M, Vergara J et al (2010) Nutrition facts and functional potential of quinoa (*Chenopodium quinoa* willd.), an ancient Andean grain: a review. J Sci Food Agric 90:2541–2547

Vilcacundo R, Martínez-Villaluenga C, Hernández-Ledesma B (2017) Release of dipeptidyl peptidase IV, α-amylase and α-glucosidase inhibitory peptides from quinoa (*Chenopodium quinoa* Willd.) during in vitro simulated gastrointestinal digestion. J Funct Foods 35:531–539. https://doi.org/10.1016/j.jff.2017.06.024

Vilcacundo R, Miralles B, Carrillo W, Hernández-Ledesma B (2018) In vitro chemopreventive properties of peptides released from quinoa (*Chenopodium quinoa* Willd.) protein under simulated gastrointestinal digestion. Food Res Int 105:403–411. https://doi.org/10.1016/j.foodres.2017.11.036

Wan Y, Shang J, Graham R et al (2020) Receptor recognition by the novel coronavirus from Wuhan: an analysis based on decade-long structural studies of SARS coronavirus. J Virol 94:127–147. https://doi.org/10.1128/jvi.00127-20

Wang J, Xiao J, Liu X et al (2019) Analysis of tartary buckwheat (*Fagopyrum tataricum*) seed proteome using offline two-dimensional liquid chromatography and tandem mass spectrometry. J Food Biochem 43:1–9. https://doi.org/10.1111/jfbc.12863

Wu C, Liu Y, Yang Y et al (2020) Analysis of therapeutic targets for SARS-CoV-2 and discovery of potential drugs by computational methods. Acta Pharm Sin B10:766–788. https://doi.org/10.1016/j.apsb.2020.02.008

Xiao X, Chakraborti S, Dimitrov AS et al (2003) The SARS-CoV S glycoprotein: expression and functional characterization. Biochem Biophys Res Commun 312:1159–1164. https://doi.org/10.1016/j.bbrc.2003.11.054

Xu H, Zhong L, Deng J et al (2020) High expression of ACE2 receptor of 2019-nCoV on the epithelial cells of oral mucosa. Int J Oral Sci 12:1–5. https://doi.org/10.1038/s41368-020-0074-x

Xu X, Chen P, Wang J et al (2020) Evolution of the novel coronavirus from the ongoing Wuhan outbreak and modeling of its spike protein for risk of human transmission. Sci China Life Sci 63:457–460

Yang N, Li YM, Zhang K et al (2014) Hypocholesterolemic activity of buckwheat flour is mediated by increasing sterol excretion and down-regulation of intestinal NPC1L1 and ACAT2. J Funct Foods 6:311–318. https://doi.org/10.1016/j.jff.2013.10.020

Zhang H, Penninger JM, Li Y et al (2020) Angiotensin-converting enzyme 2 (ACE2) as a SARS-CoV-2 receptor: molecular mechanisms and potential therapeutic target. Intensive Care Med 46:586–590. https://doi.org/10.1007/s00134-020-05985-9

Zhu F (2016) Chemical composition and health effects of Tartary buckwheat. Food Chem 203:231–245. https://doi.org/10.1016/j.foodchem.2016.02.050